

Q^2 Measurement and Challenges in PREX

Kiadtisak Saenboonruang^{1,2,*} and Nilanga Liyanage²

ABSTRACT

The four-momentum transfer squared (Q^2) is an important kinematic quantity for nuclear experiments. The importance of the Q^2 measurement was emphasized in the case of PREX, conducted at Hall A, Jefferson Lab, which measured the parity-violating electroweak asymmetry in the elastic scattering of polarized electrons off a ^{208}Pb target against an average Q^2 in order to find the neutron radius. With the requirement of 1% uncertainty in Q^2 , the measurement became extremely challenging with the need to find new solutions and techniques to overcome several constraints including the use of a low electron beam current, the limited capabilities of the existing equipment and the design of the experiment (a 5° central scattering angle). With a new technique using the idea of differential nuclear recoil for elastic electron scattering off target nuclei of different masses to measure the spectrometer central angle (θ_0) and scattering angle (θ) for Q^2 calculation, the average Q^2 was measured to be $0.00906 \pm 0.00009 \text{ GeV}^2$, which was within the 1% uncertainty requirement of the experiment. This article summarizes all procedures and challenges of Q^2 measurement in PREX and possible improvement for future PREX-like experiments.

Keywords: Q^2 measurement, Jefferson Lab, PREX, parity violation, neutron radius

INTRODUCTION

The four-momentum transfer squared (Q^2) is the square of the amount of momentum transfer from one particle to another particle in four-dimensional space. The Q^2 plays an important role in the kinematic parts of nuclear experiments and usually defines the accuracy of experiments and is calculated using Equation 1

$$Q^2 = 2EE' [1 - \cos(\theta)] \quad (1)$$

where E is the incident energy, E' is the energy of scattered electrons and θ is the scattering angle. In the case of elastic electron scattering, one may eliminate one of the three variables and the Q^2

can be written as in Equations 2–4 (for a proton target):

$$Q^2 = 2E^2 f_r [1 - \cos(\theta)] \quad (2)$$

$$Q^2 = 2E'^2 f_r' [1 - \cos(\theta)] \quad (3)$$

$$Q^2 = 2m_p(E - E') \quad (4)$$

where m_p is the mass of the proton, f_r and f_r' are recoil factors defined as shown in Equations 5 and 6:

$$f_r = \frac{1}{1 + \left(\frac{E}{M}\right) [1 - \cos(\theta)]} \quad (5)$$

¹ Department of Applied Radiation and Isotopes, Faculty of Science, Kasetsart University, Bangkok 10900, Thailand.

² Physics Department, University of Virginia, Charlottesville, VA 22903, USA.

* Corresponding author, e-mail: fscikssa@ku.ac.th

$$f_r = \frac{1}{1 + \left(\frac{E'}{M}\right)[1 - \cos(\theta)]} \quad (6)$$

where M is the mass of target nuclei. For PREX, Equation 1 was the primary equation used in Q^2 calculation, while Equations 2 and 3 were used for consistency checking. Equation 4 was not used for the Q^2 calculation due to the high uncertainty arising from the small differences in $E-E'$.

The importance of the Q^2 was greatly enhanced in PREX (Abrahamyan *et al.*, 2012) since the experiment measured the parity-violating electroweak asymmetry in the elastic scattering of polarized electrons off a ^{208}Pb target against an average Q^2 measured throughout the experiment. In order to achieve the proposed goal of 3% accuracy in neutron radius measurement, the accuracy of the Q^2 measurement must be better than 1%. This requirement was extremely challenging for the experiment because new techniques and solutions were needed to overcome all constraints, which included the limited capabilities of existing tracking devices. The usual trackers in Hall A, Jefferson Lab, Newport News, VA, USA are sets of Vertical Drift Chambers (VDCs) (Alcorn *et al.*, 2004). Even though the VDCs have been used successfully and efficiently for many nuclear experiments in the past, the ability to handle high event rates is limited. Since PREX measures the scattered electrons at 5° off a ^{208}Pb target, the rates of scattered electrons at the drift chambers (up to 50--MHz/cm^2) were well beyond the normal operational limit of the VDCs, which is $\sim 10\text{ kHz/cm}^2$. With such high event rates in PREX, the performance of the VDCs would be reduced substantially and could possibly lead to a large amount of uncertainty in Q^2 measurement. Another constraint was the use of a low electron beam current. To cope with too high event rates at the VDCs, PREX uses a low electron beam current ($\sim 50\text{ nA}$) during the Q^2 measurement to reduce the event rates at VDCs. However, with a low electron beam current, the beam position monitors and the

beam position locks do not function properly. The lack of these two pieces of equipment could lead to possible beam fluctuations that directly affect the Q^2 measurement.

Several new techniques and thorough analyses were performed to ensure the accuracy of the Q^2 measurement satisfied the requirement of PREX.

METHODOLOGY

Components of Q^2 measurement

From Equation 1, the quantities needed for Q^2 measurement consist of the incident electron beam energy (E), the scattered electron beam energy (E'), and the scattering angle (θ).

Beam energy (E) measurement

The nominal beam energy for PREX was 1.063 GeV and was continuously measured by the Tiefenbach measurement (Riordan, 2008), which had been calibrated using two independent apparatus, ARC (Gougnous *et al.*, 1999) and eP (Ravel, 1998), which are accurate to the level of 3×10^{-4} . However, since PREX only used the Tiefenbach measurement for beam energy measurement, the accuracy was limited to $\sim 0.1\%$ level and contributed $\sim 0.1\%$ to the overall systematic uncertainty in Q^2 .

Scattered electron energy (E') measurement

The scattered electron energy was measured using two high resolution spectrometers (LHRS and RHRS) in Hall A. (Alcorn *et al.*, 2004) The standard HRS has an absolute energy accuracy in the range $\sim 3 \times 10^{-4}$ for the energy of 0.3–0.4 GeV. However, since PREX measured the central scattering angle of 5° while the smallest angle the HRSs could have was 12.5° , a new septum magnet that bent scattered electrons from 5° to 12.5° had to be installed. The addition of the septum magnet led to the need to recalibrate both HRSs. The recalibration procedures are described in Saenboonruang (2013). The final accuracy was

found to be better than 0.1% level and contributed ~0.1% to the overall systematic uncertainty in Q^2 .

Scattering angle (θ) measurement

The scattering angle (θ) is the angle between the direction of a scattered electron and the direction of the electron beam. θ can be divided into two main parts: the spectrometer central angle (θ_0) and angles measured with respect to the spectrometer axis called target angles (θ_{tg} and ϕ_{tg} where θ_{tg} (ϕ_{tg}) is a vertical (horizontal) angle of scattered electrons with respect to the spectrometer axis). For a small scattering angle, θ is related to θ_0 , θ_{tg} and ϕ_{tg} as shown in Equation 7. Figure 1 shows how each variable is defined in the spectrometer.

$$\theta = \frac{\cos(\theta_0) - \phi_{tg} \sin(\theta_0)}{\sqrt{1 + \theta_{tg}^2 + \phi_{tg}^2}} \quad (7)$$

The uncertainty from measuring the scattering angle was the main uncertainty that contributed to the overall systematic uncertainty in Q^2 , especially the uncertainty from the θ_0 measurement.

Spectrometer central angle (θ_0) measurement

θ_0 can be measured using a **survey**, which

measures the angle between two imaginary lines. The first line is along the ideal spectrometer axis and the second line is along the ideal electron beam direction. A survey uses special equipment from the Stanford Industrial Measurement System (SIMS) (Bell, 1989) to locate positions of the target center and the ideal spectrometer center. However, multiple transformations required to relate the ideal spectrometer angle to the actual spectrometer angle could increase the uncertainty of θ_0 measurement to be as much as 0.06° or ~1%, which could lead to 2% uncertainty in Q^2 measurement in the case of PREX.

However, PREX used a new technique in addition to a survey. This technique (called pointing measurement) makes use of the idea of differential nuclear recoil for elastic electron scattering off target nuclei of different masses. The accuracy achieved from pointing measurement is usually better than a survey since pointing measurement does not require multiple transformations as in the case of a survey. Moreover, the accuracy of pointing measurement can be greatly enhanced by considering differential nuclear recoil off different target nuclei that are in the same target such as water (H_2O). The benefit of this method is that all uncertainties from estimating energy

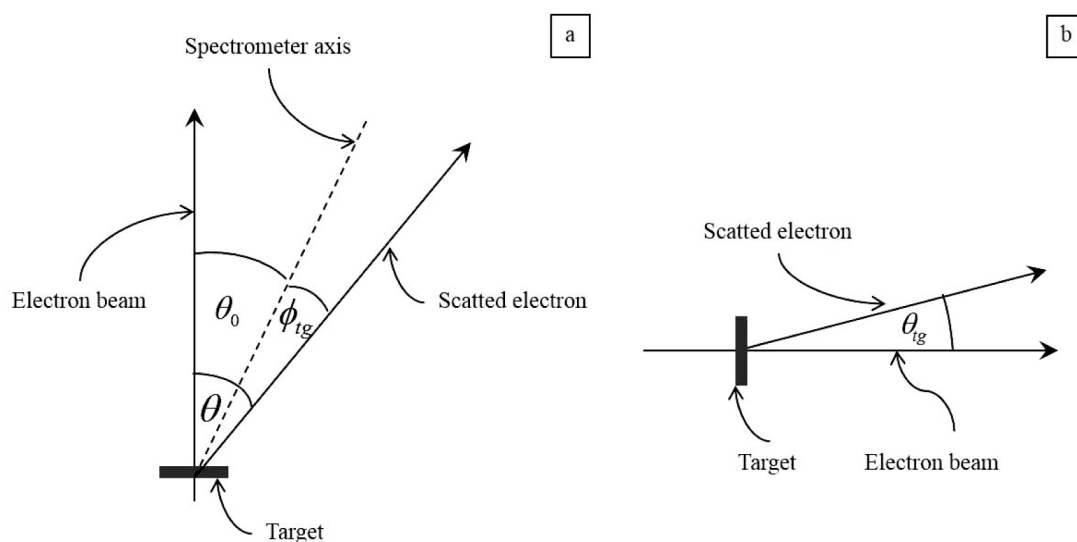


Figure 1 Relationship between scattering angle (θ), spectrometer central angle (θ_0) and spectrometer reconstruction angle (target angle, θ_{tg} and ϕ_{tg}): (a) Top view; (b) Side view.

losses that occurred before and after the scattering are suppressed. Also, by following this method, the problem of possible beam position shifting during the run is eliminated. The main uncertainty contributed to the uncertainty of a pointing measurement is from the ability to measure the energy difference between two different peaks, which, in the case of PREX, had an accuracy at the level of ~ 30 keV. Procedures for the pointing measurement are described in Saenboonruang (2013).

For PREX, θ_0 for both HRSs obtained from a survey and a pointing measurement are shown in Table 1 and Figure 2.

As shown in Table 1 and Figure 2, the accuracy of θ_0 measurement obtained from the pointing measurement was improved by a factor of two compared to values obtained from the survey. The improved accuracy from the pointing measurement helped to reduce the overall uncertainty of the Q^2 measurement to within the 1% requirement.

Measurement of target angles (θ_{tg} and ϕ_{tg})

After the θ_0 measurement, the Q^2 could be measured with the required accuracy at the scattering angle of θ_0 . However, PREX used the average Q^2 from the entire acceptance of spectrometers to measure the neutron radius. Hence, scattered electrons that deviated from the spectrometer axes must be calibrated in order to have the correct θ_{tg} and ϕ_{tg} . The procedures are called optics calibration (Liyanage, 2002), which links focal plane variables to target variables. Uncertainties for θ_0 , θ_{tg} , and ϕ_{tg} measurement are shown in Table 2.

Combining all uncertainties from θ_0 , θ_{tg} , and ϕ_{tg} measurement, the average systematic uncertainty from scattering angle (θ) measurement would be 0.024° for LHRS and 0.021° for RHRS. The 0.4% uncertainty in scattering angle (θ) measurement, as shown in Table 3, contributed $\sim 0.9\%$ to the overall systematic uncertainty in Q^2 .

Table 1 Spectrometer angles, θ_0 , measured using pointing method and survey method of PREX.

High resolution spectrometer (HRS)	Pointing values ($^\circ$)	Survey values ($^\circ$)
Left-HRS (LHRS)	5.065 ± 0.020	5.007 ± 0.046
Right-HRS (RHRS)	4.933 ± 0.020	4.910 ± 0.046

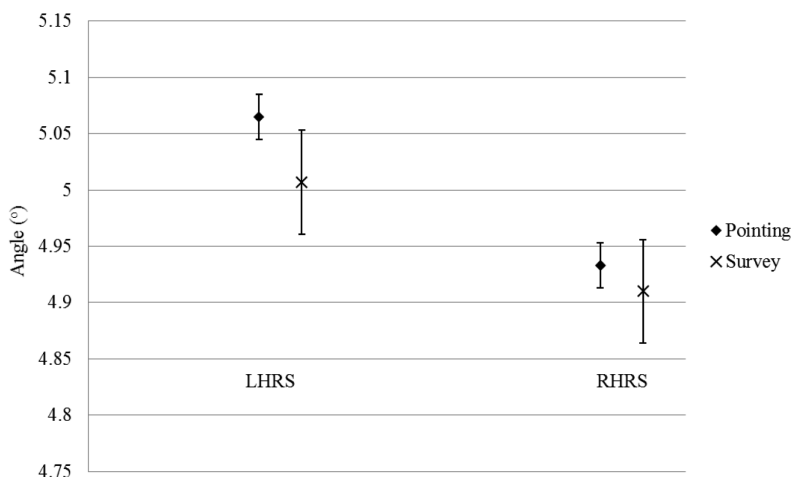


Figure 2 Comparison of spectrometer central angles, θ_0 , on two high resolution spectrometers (LHRS and RHRS) using pointing measurement and survey. The error bars (\pm SD) show a smaller uncertainty from using pointing measurement.

Measurement of Q^2

During the production runs, which used a higher beam current ($\sim 50\text{--}100\ \mu\text{A}$) in order to shorten the experiment time required to achieve sufficient data, all the VDCs were turned off due to the too high scattered electron flux on the detectors. Thus, no Q^2 data were recorded during the production runs. As a consequence, in order to measure the average Q^2 , a series of Q^2 runs was taken approximately once a week with a lower beam current ($\sim 50\ \text{nA}$).

In order to ensure that the Q^2 values would represent scattered electrons that passed through the main PREX detectors, the scattered electrons must hit both the main PREX detectors and have non-zero ADC amplitudes after pedestal subtraction. Then, the information about target angles, electron beam energy and scattered electron energy for each detected electron was recorded and was used to calculate Q^2 using Equation 1. The average Q^2 values obtained from every scattered electron that passed the cut in each run were used to calculate the final average Q^2 . The Q^2 distributions on runs from both HRSs are shown in Figure 3. The average Q^2 for LHRS was $0.00933 \pm 0.00009\ \text{GeV}^2$, while the average Q^2 for RHRS was $0.00875 \pm 0.00009\ \text{GeV}^2$. The different values of Q^2 in each spectrometer were consistent with the different spectrometer central angles (θ_0) (larger θ_0 led to higher Q^2).

To obtain the final average of Q^2 from both spectrometers, the relative strengths or the

weights between the left PREX detectors and the right PREX detectors must be determined. Even though the PREX detectors on both HRSs were tuned through high voltage (HV) adjustments periodically such that their gains were kept roughly equal, there were still some small imbalances. By using the average ratio of ADC amplitudes from the left and right PREX detectors from all Q^2 runs, the relative strengths could be obtained. The calculation yielded the weights of 0.5020 and 0.4980 for LHRS and RHRS respectively. The value of the final average of Q^2 from the two spectrometers after the corrections was $0.00906\ \text{GeV}^2$.

RESULTS AND DISCUSSION

Shifts in Q^2 between runs

As shown in Figure 3, there were some shifts in Q^2 by as much as 1% between runs. These shifts could be explained by the shifts in average beam positions for detected events, which could be due to two main reasons: 1) After taking the beam for several days, some parts of the target melted away and became non-uniform. This reduced the yield for those thinner parts and, with the beam raster on, the average beam position seen by the detectors changed. 2) Due to the low beam currents during Q^2 runs, the beam position locks were not in place. This may have caused the actual beam position to change.

Table 2 Uncertainties of θ_0 , θ_{tg} , and φ_{tg} measurement.

High resolution spectrometer (HRS)	Uncertainty of θ_0 ($^\circ$)	Uncertainty of θ_{tg} ($^\circ$)	Uncertainty of φ_{tg} ($^\circ$)
Left-HRS (LHRS)	0.020	0.066	0.017
Right-HRS (RHRS)	0.020	0.091	0.011

Table 3 Uncertainties of scattering angles (θ).

High resolution spectrometer (HRS)	Uncertainty of θ ($^\circ$)	Relative uncertainty of θ (%)
Left-HRS (LHRS)	0.024	0.4
Right-HRS (RHRS)	0.021	0.4

The change in beam position to one side would increase Q^2 on one spectrometer and decrease Q^2 on the other spectrometer. Since the beam position monitors did not operate during Q^2 runs due to the low beam current (~ 50 nA), the beam position was extracted using the measured y_{tg} instead. Consider Equation 8:

$$Z_{react} = -(y_{tg} + D) \frac{\cos(\phi_{tg})}{\sin(\theta_0 + \phi_{tg})} + x_{beam} + x_{beam} \cot(\theta_0 + \phi_{tg}) \quad (8)$$

where Z_{react} , D , and x_{beam} are the interaction position along the beam, the horizontal displacement

of the spectrometer axis from its ideal position and the horizontal beam position at the target, respectively. Since PREX used a very thin (~ 0.55 g/cm²) ^{208}Pb target, Z_{react} was negligible, x_{beam} could be extracted directly from y_{tg} , given that y_{tg} was properly calibrated and D was accurately measured. Figures 4 and 5 illustrate how the measured Q^2 values changed as the beam average beam position shifted. This result agreed with the assumption that when the average beam position moved to one side, Q^2 on one spectrometer increased while on the other spectrometer it decreased.

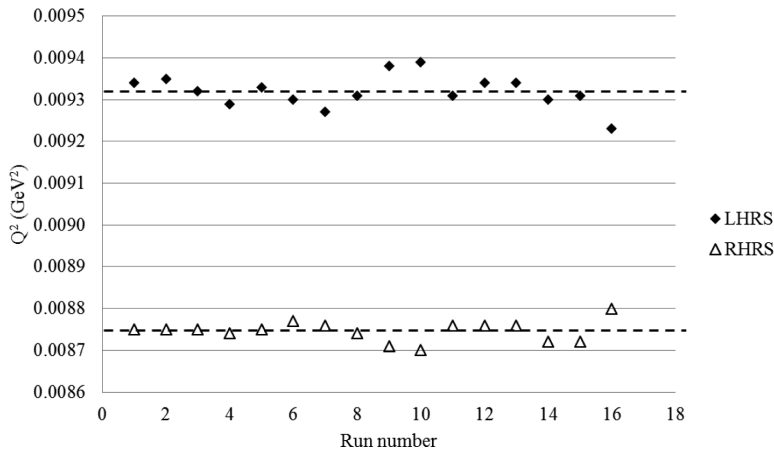


Figure 3 Q^2 distributions on runs from both high resolution spectrometers (LHRs and RHRS). The dotted lines represent the average Q^2 for each spectrometer.

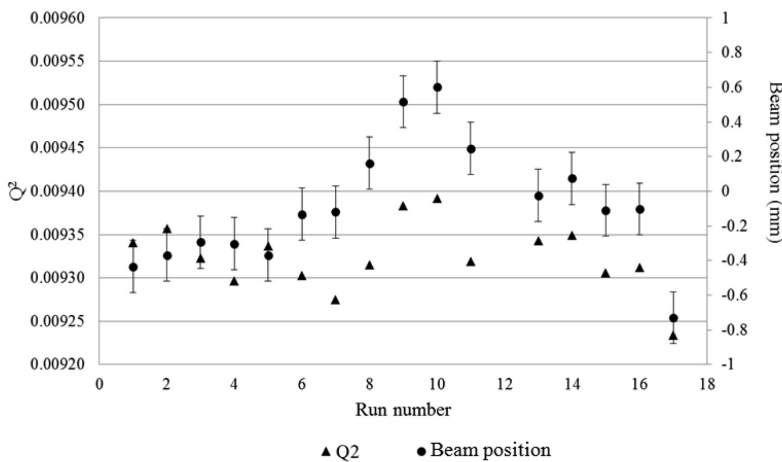


Figure 4 Q^2 distributions versus beam positions on the left high resolution spectrometer (LHRs). Error bars show \pm SD.

Other systematic uncertainties on the Q^2 measurement

Pileup

Pileup effects occurred from running the experiment at too high trigger rates which substantially decreased the performances of the VDCs. To determine the size of a pileup, a series of Q^2 runs were taken with trigger rates varying over a large range from 300 Hz to 500 kHz, and the VDC performances were determined from the Q^2 distributions. Figures 6 and 7 clearly show the pileup occurred when the trigger rates were high (500 kHz).

Figure 8 shows how the average value of Q^2 obtained from different trigger rates changed.

To reduce the effect of pileup on the Q^2 measurement, only Q^2 runs with trigger rates lower than 100 kHz were used. However, even at lower trigger rates, pileup effects could still occur. The effect could be estimated by comparing Q^2 for different cuts on the number of tracks in the event. Using a 1-track only cut versus allowing multiple tracks on the detector resulted in an average shift of $-0.06 \pm 0.05\%$ on Q^2 . This shift in Q^2 values was taken as a systematic uncertainty arising from pileup effects.

Trigger bias

PREX used two types of trigger: T1 and T5. T1 was the scintillator above the VDC planes,

while T5 was the scintillator placed just above the main PREX detectors and was used as the main trigger during the Q^2 measurement. By comparing the Q^2 values collected from the same run but using different trigger types, T5 gave Q^2 values $\sim 0.2\%$ higher than the Q^2 values obtained from the T1 triggered events. The difference in the Q^2 using two different trigger types could be regarded as a systematic uncertainty arising from trigger bias.

Q^2 result and its systematic uncertainties

Summaries of Q^2 and its uncertainties are shown in Tables 4 and 5.

Possible improvements for future PREX-like experiments

PREX was one of the very first experiments at JLAB that was run with a very small forward angle (5° central scattering angle) and with heavy target nuclei (^{208}Pb), which led to a tiny value of measured Q^2 . With constraints on the low beam current (~ 50 nA) during the Q^2 measurement and the limitation on the equipment capability in PREX, a few improvements could be made for future PREX-like experiments in order to improve the accuracy of the Q^2 measurement.

Use of a Gas Electron Multiplier detector

The Gas Electron Multiplier (GEM) detector is a relatively new gaseous detector

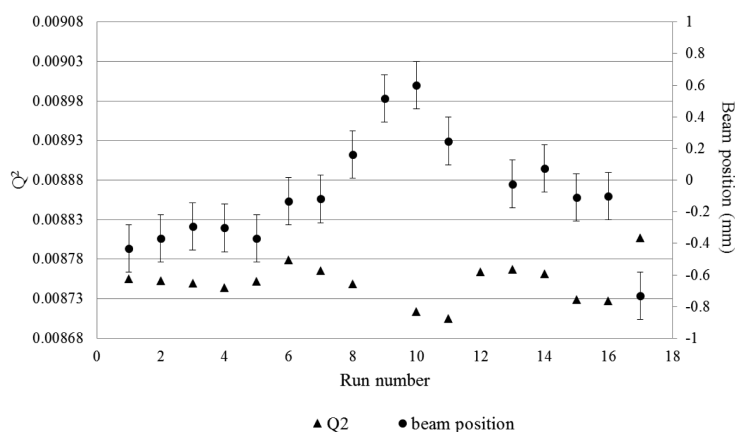


Figure 5 Q^2 distributions versus beam positions on the right high resolution spectrometer (RHRS). Error bars show \pm SD.

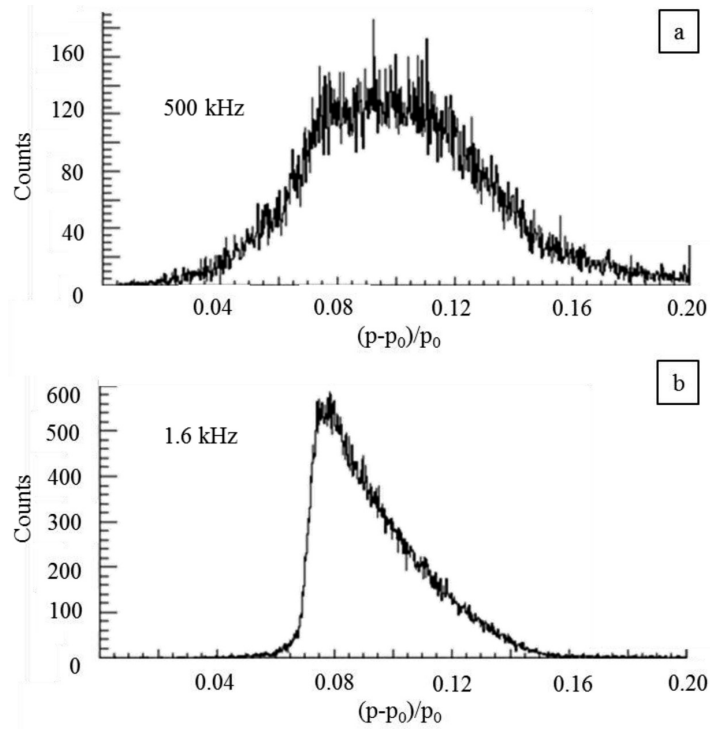


Figure 6 Q^2 distributions in the high resolution spectrometer LHRS with: (a) Very high trigger rate (500 kHz) clearly showing pileup; (b) Low trigger rate (1.6 kHz).

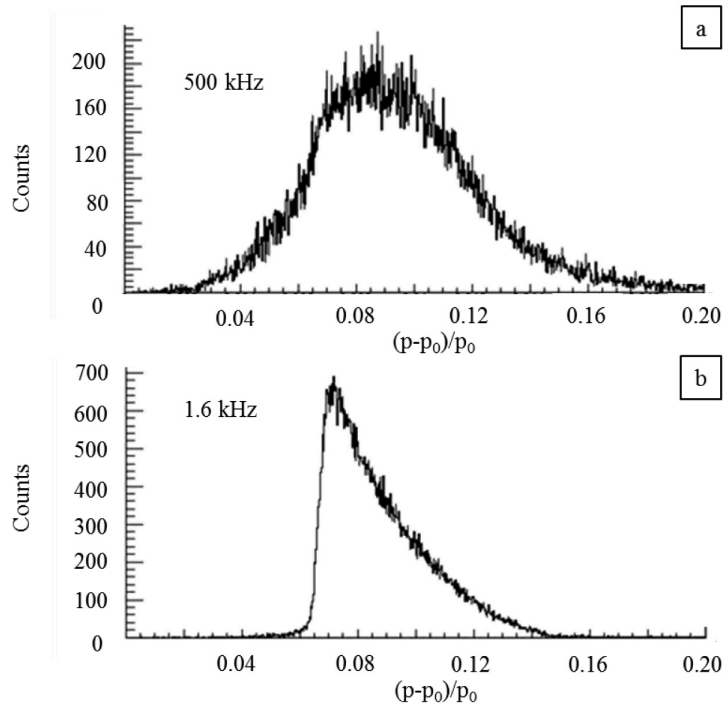


Figure 7 Q^2 distributions in the high resolution spectrometer RHRS with: (a) Very high trigger rate (500 kHz) clearly showing pileup; (b) low trigger rate (1.6 kHz).

introduced by Sauli (1997). The GEM detector uses the principle of ionization of gas molecules inside the detector caused by particles going through the detector. These primary ionized

electrons will be accelerated toward the cascaded GEM foils, which consist of arrays of small holes (diameter $\sim 70\ \mu\text{m}$), and gain more energy. These higher-energy electrons will be able to ionize more

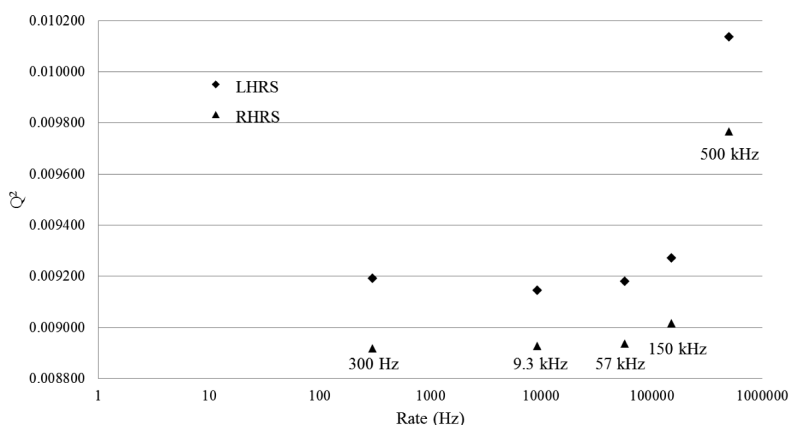


Figure 8 Q^2 dependence on trigger rates on the two high resolution spectrometers (LHRS and RHRS).

Table 4 Summary of Q^2 and useful information for PREX.

Quantity	Values
Beam energy (GeV)	1.063±0.001
LHRS θ_0 ($^\circ$)	5.065±0.024
RHRS θ_0 ($^\circ$)	4.933±0.021
Average Q^2 on LHRS (GeV 2)	0.00933±0.00009
Average Q^2 on RHRS (GeV 2)	0.00875±0.00009
LHRS Q^2 weight	0.5020±0.0005
RHRS Q^2 weight	0.4980±0.0005
Average Q^2 (GeV 2)	0.00906±0.00009

LHRS, RHRS = High resolution spectrometers.

Values are shown as mean±SD.

Table 5 Summary of uncertainties in Q^2 measurement for PREX.

Uncertainty source	Uncertainty (in source units)	Percent uncertainty in Q^2
Beam energy	1 MeV	0.1%
Scattered electron energy	1 MeV	0.1%
Scattering angle	0.023 $^\circ$	0.9%
Pileup		<0.1%
Trigger bias		0.2%
Total systematic uncertainty		1.0%
Statistical uncertainty		<0.1%
Total uncertainty		1.0%

electrons in later stages of amplification, creating an electron avalanche. The readout plane at the bottom of the detector will capture this electron avalanche for further signal analysis. The working principle of the GEM detector is shown in Figure 9.

Since its invention in 1997, the GEM detector has been used and developed in various fields of research and has been excellent from many perspectives. In particular, the GEM detector could be a perfect candidate to replace the VDCs for Q^2 measurement because of its characteristics of: high rate of detection capability (up to 10^5 Hz/mm²); position resolution of better than 70 μ m; radiation hardness; effective gain of $\sim 10^4$; adaptability in size and shape for different applications; and low discharge probability (Sauli, 2004).

The high rate of detection capability in the GEM detector will enable PREX-like experiments to be run at a much higher beam current. This will also allow beam position monitors and beam position locks to properly function, while still ensuring position resolution and energy proportionality. The ability to monitor and lock the beam will reduce the possibility of beam shifts during runs and reduce the overall systematic uncertainty.

Low-current beam position monitoring system

In addition to the possibility of using the GEM detector for higher beam current, a low-current beam position monitoring system could be applied as well. The low-current beam position monitoring system has been developed in Hall B,

Jefferson Lab to measure the transverse position of a very low current (in nA scale) beams delivered to Hall B (Ursie, 1997). The success in using the low-current beam position monitoring system will reduce the fluctuations in the beam position during runs and substantially reduce the systematic uncertainty for the Q^2 measurement.

CONCLUSION

The Q^2 was successfully measured with an overall uncertainty of 1%, despite major challenges in the use of a low beam current and a small scattering angle. The uncertainty of 1% in the Q^2 measurement was within the requirement of the experiment in order to extract a proposed 3% accuracy in neutron radius measurement. The main uncertainty was from measuring the spectrometer central angle (θ_0), with pointing measurement ensuring the required accuracy was achieved. In addition, there were some shifts in Q^2 by as much as 1% during runs due to shifts in beam positions. Despite the success in the measurement, there is still room for improvement. Some possible improvements include the use of GEM detectors to replace VDCs and the utilization of a low-current beam position monitoring system.

ACKNOWLEDGEMENTS

The authors would like to thank: all staff at Jefferson Lab, especially the PREX collaborators, for their help in planning, setting up,

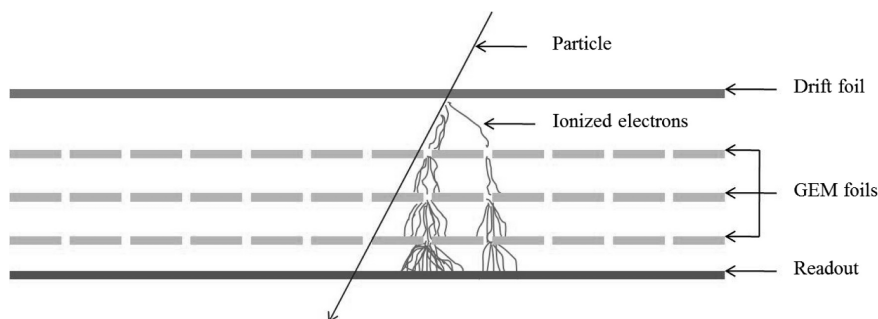


Figure 9 Schematic of working principles of the Gas Electron Multiplier (GEM) detector.

collecting data and analysis; the US Department of Energy and Jefferson Lab for support; and special thanks are recorded to Dr. Robert Michaels for help and advice on performing the Q^2 analysis.

LITERATURE CITED

- Abrahamyan, S., *et al.* 2012. Measurement of the neutron radius of ^{208}Pb through parity violation in electron scattering. **Phys. Rev. Lett.** 108: 112502.
- Alcorn, J., *et al.* 2004. Basic instrumentation for Hall A at Jefferson Lab. **Nucl. Instr. and Meth. A.** 522 (3): 294–346.
- Bell, B., 1989. SIMS: The SLAC Industrial Measurement System. *In Proceedings of the 1st International Workshop on Accelerator Alignment (IWAA 1989)*: 162–170. [Available from: <http://www.slac.stanford.edu/econf/C8907312/papers/012.PDF>]. [Sourced: September 24, 2014].
- Curtis, C., J. Dahlberg, W. Oren and K. Tremblay. Techniques used in the alignment of TJNAF's accelerators and experimental halls. *In Proceedings of the 5th International Workshop on Accelerator Alignment (IWAA 1997)*. 038. [Available from: <https://www.jlab.org/eng/survalign/documents/publ/CCurt97.pdf>]. [Sourced: September 22, 2014].
- Gouгнаus, F., A. Donati, J. Fabre, F. Kircher, Y. Lussignol, J. Marroncle, G. Matichard, D. Marchand, J.C. Sellier, P. Vernin and C. Veyssiere. 1999. Controls for high precision beam energy determination at CEBAF, Hall A: The ARC project. *In Proceedings of International Conference on Accelerator and Large Experimental Physics Control Systems*. Trieste, Italy: 45–47. [Available from: <http://cds.cern.ch/record/532637/files/wc1p06.pdf>]. [Sourced: September 24, 2014].
- Liyanage, N. 2002. **Optics Calibration of the Hall A High Resolution Spectrometers Using the New Optimizer**. [Available from: <http://hallaweb.jlab.org/publications/Technotes/files/2002/02-012.pdf>]. [Sourced: 22 September 22, 2014].
- Ravel, O., *et al.* 1998. Beam energy measurement at TJNAF at a level of $\Delta E/E=10^{-4}$ by determination of the $p(e,e'p)$ kinematics on hydrogen. **Nucl. Instr. and Meth. A.** 409: 611–612.
- Riordan, S.P. 2008. **Measurement of the Electric form Factor of the Neutron at Four-Momentum Squared**. PhD. thesis. Carnegie Mellon University, Pittsburgh, PA, USA. [Available from: <http://search.proquest.com/docview/304666813>]. [Sourced: September 24, 2014].
- Saenboonruang, K., 2013. **Measurement of the Neutron Radius of ^{208}Pb Through Parity Violation in Electron Scattering**. PhD. thesis. University of Virginia, Charlottesville, VA USA. [Available from: <http://hallaweb.jlab.org/parity/prex/theses/KiadtisakThesis.pdf>]. [Sourced: September 24, 2014].
- Sauli, F., 1997. GEM: A new concept for electron amplification in gas detectors. **Nucl. Instr. and Meth. A.** 386 (23): 531–534.
- Sauli, F., 2004. Progress with the Gas Electron Multiplier. **Nucl. Instr. and Meth. A.** 522: 93–98.
- Ursie, R., R. Flood, C. Piller, E. Strong and L. Turlington, 1997. 1 nA beam position monitoring system. *In Proceedings of Particle Accelerator Conference, Vol. 2*. 2: 2131–2133. [Available from: <http://accelconf.web.cern.ch/accelconf/pac97/papers/pdf/9P089.PDF>]. [Sourced: September 24, 2014].